Dipolar and Bond Vector Correlation Function of Linear Polymers Revealed by Field Cycling ^{1}H NMR: Crossover from Rouse to Entanglement Regime

A. Herrmann,[†] V. N. Novikov,[‡] and E. A. Rössler*,[†]

Experimentalphysik II, Universität Bayreuth, 95440 Bayreuth, Germany, and IA&E, Russian Academy of Sciences, Novosibirsk, 630090, Russia

Received December 18, 2008; Revised Manuscript Received January 15, 2009

ABSTRACT: We apply field cycling NMR to study segmental reorientation dynamics in melts of linear 1,4-polybutadiene (PB) in the entanglement regime ($M \geq M_e$). Dispersion data of the spin−lattice relaxation time $T_1(\omega)$ are transformed to the susceptibility representation $\chi''(\omega) = \omega/T_1(\omega)$, and using frequency temperature superposition master curves $\chi''(\omega\tau_s)$ are constructed which reflect spectral contributions from glassy as well as polymer specific dynamics. The correlation time τ_s is determined by glassy dynamics. Transforming $\chi''(\omega\tau_s)$ into the time domain and studying the crossover from Rouse to entanglement regime, the full dipolar or segmental reorientational correlation function $F_2(t/\tau_s)$ is presented covering six decades in amplitude and 8 decades in time. Assuming $F_2(t) \cong \langle \boldsymbol{u_b}(t)\boldsymbol{u_b}(0)\rangle^2$ the bond vector correlation function $\phi_b(t) = \langle \boldsymbol{u_b}(t)\boldsymbol{u_b}(0)\rangle$ is obtained. Reaching $Z = M/M_e \leq 9$, comparison with theoretical predictions by the tube-reptation model as well as renormalized Rouse theory reveals significant discrepancies whereas good agreement is found with simulations. The crossover to entanglement dynamics appears to be very protracted.

1. Introduction

The dynamics of polymer melts comprises both polymer specific dynamics as well as glassy dynamics. Whereas "polymer dynamics" originate from collective dynamics of Rouse and reptation type,[1] glassy dynamics[2−4] are attributed to "segmental" or "local" relaxation of the polymer chain. However, one has to keep in mind that the glass transition phenomenon itself includes cooperative motion with a dynamic correlation length presumably on the order of 1−10 nm. Regarding the interplay of polymer and glassy dynamics, detailed information is provided by molecular dynamics simulation.[5,6] Considering the mean square displacement of an (inner) monomer in a nonentangled chain, a crossover from the initial ballistic behavior to a plateau region is identified and attributed to the cage effect, the latter being well described by the mode coupling theory of the glass transition.[7] At longer times polymer specific subdiffusive behavior sets in which is described by Rouse theory, and finally at longest times normal diffusive behavior of the entire polymer is observed. Thus, regarding monomer relaxation only beyond the time scale of cage formation polymers and simple liquids substantially differ, and one can identify the segmental correlation time τ_s with the time scale of the α-process characterizing glassy dynamics. The latter drives the polymer dynamics via controlling the monomeric friction coefficient.

The present publication is part of a series of papers readdressing the analysis of fast field cycling (FFC) NMR data for linear polymer melts.[8,9] Preliminary results have been reported in ref 10. In the preceding work we have argued that, in order to properly access quantitative aspects of the spectral contributions due to polymer specific dynamics, the generally much stronger contribution of glassy dynamics has to be accounted for. As a first approach, assuming statistical independence and time scale separation the individual contributions to the total spectrum have been taken to be additive and "polymer spectra" have been obtained by subtracting the "glassy spectrum" from the overall spectrum. The integral over the polymer spectrum with respect to the total spectrum then provides a measure of the polymer relaxation strength. The so obtained polymer spectra significantly differ from the overall spectra in the case of Rouse dynamics of nonentangled polymers, i.e. when moderately long chain lengths are considered. In this regime, the glass transition temperature T_g is a function of M,[11] and thus the spectra have to be rescaled by τ_s to provide "iso-frictional" spectra which allow comparison among polymers with different M.[8,9]

The separation of glassy dynamics and Rouse dynamics may be challenged as in a strict sense time scale separation leading to an additive decomposition is only partly given. The situation is less severe in the entanglement regime, i.e., above M_e, as in this case time scales of glassy and slow entanglement dynamics are well separated. Moreover, for polymers with comparably high polymer relaxation strength the situation becomes even more favorable. Here, we again have chosen polybutadiene (PB) which has turned out to exhibit strong polymer relaxation.[9] Thus, without attempting the above-described decomposition we will analyze the full dipolar or segmental correlation function obtained from transforming the T_1 dispersion data into the time domain. Further, $T_1(\omega)$ data can be converted into the bond vector correlation function which will be compared to simulations.[12,13] By adding further experimental data to our previous results[8,9] for PB in the range $M > M_e$ the segmental correlation function extending up to 8 decades in time will be presented, containing now contributions from both glassy and polymer dynamics. Relying on these time domain data we will analyze the terminal relaxation for the crossover from the Rouse to the entanglement regime, an alternative approach to the one taken before by analyzing FFC NMR data in the susceptibility representation.[9] Finally, the extracted segmental as well as the bond vector correlation function will be discussed in the light of theoretical predictions. Reaching $Z = M/M_e \cong 9$, it will turn out that standard polymer theories are inappropriate to describe our results; however, good agreement is found with simulation data.[12]

2. Theoretical Background

The spin−lattice relaxation time T_1 describes the evolution of the macroscopic nuclear magnetization toward its equilibrium

* Corresponding author.
[†] Experimentalphysik II, Universität Bayreuth.
[‡] IA&E, Russian Academy of Sciences.

10.1021/ma802818j CCC: $40.75
Published on Web 02/20/2009

Table 1. Details on the Samples

sample	M_w [g/mol]	M_w/M_n
PB816	816	1.05
PB9470	9470	1.02
PB18000	18000	1.05
PB35300	35300	1.02

value. Its frequency dependence (or dispersion) may be studied by applying the FFC technique where the external magnetic field is switched between a variable relaxation field B and a constant detection field. The angular frequency is defined by the Larmor frequency $\omega = \gamma B$ where γ denotes the gyromagnetic ratio of the nucleus. In the case of ^{1}H nuclei the evolution of the spin−lattice relaxation is determined by fluctuations of the dipolar interaction among the proton spins, and T_1 is dominated by intramolecular contributions but intermolecular correlation may also play a role. In the case of polymers, direct comparison of ^{1}H and ^{2}H NMR relaxation data indicate that indeed intermolecular translation dynamics may show up at very low frequencies in ^{1}H NMR[14] (cf. also discussion part).

In order to facilitate analyses and comparisons with other techniques we rewrite the Bloembergen, Purcell, and Pound (BPP) expression[15] for the relaxation rate $1/T_1$ in the susceptibility form[8,9]

$$\omega/T_1(\omega) = C[\chi''(\omega) + 2\chi''(2\omega)] \equiv 3C\tilde{\chi}''(\omega) \quad (1)$$

where C is the NMR coupling constant, and $\chi''(\omega) = \omega J(\omega)$ the susceptibility, with the spectral density $J(\omega)$ being given in first approximation by the Fourier transform of the correlation function $F_2(t)$ and the latter by the second rank orientational correlation function of a polymer segment, more precisely of the internuclear vectors of the spin pairs in the monomer.[9,14,15] We define a correlation function $\tilde{F}_2(t)$ given by the Fourier transform of $\tilde{\chi}''(\omega)$. As the relaxation behavior is discussed on logarithmic scales the slight difference between $\tilde{\chi}''(\omega)$ and $\tilde{\chi}''(\omega)$ as well as $\tilde{F}_2(t)$ and $F_2(t)$ can be neglected.

As a large temperature range is covered, glassy dynamics as well as polymer dynamics are probed, and one is able to construct master curves $\tilde{\chi}''(\omega\tau_s)$ for the NMR susceptibility assuming frequency temperature superposition (FTS). For that purpose we shift the susceptibility data of each temperature to achieve agreement with some suitable susceptibility function such as the Kohlrausch function on the high frequency side, i.e. at $\omega\tau_s \geq 1$ for which no polymer dynamics are observed. The shift factor yields the time constant τ_s of segmental motion, which may be identified with that of the α-process, the latter being the main relaxation of glass formers. For simple liquids, and oligomers with molecular weight $M < M_R$, there is no spectral contribution at $\omega\tau_s < 1$ in excess to the Debye behavior $\tilde{\chi}''(\omega) \propto \omega^1$, and their susceptibility master curves solely represent glassy dynamics ("glassy spectrum"). For samples with higher M, *i.e.*, $M > M_R$, additional intensity on the low frequency side of the α-peak reflects polymer specific dynamics that involve time scales longer than τ_s. We therefore have identified M_R with the molecular weight of the Rouse unit, i.e. only at $M > M_R$ Rouse modes develop.[8,9] The master curves $\tilde{\chi}''(\omega\tau_s)$ present iso-frictional spectra and allow comparing the results for different M. Alternatively, one may inspect the corresponding correlation function $\tilde{F}_2(t/\tau_s)$.

In the present contribution we refrain from separating the spectral contributions of polymer and glassy dynamics, and given that $M > M_e$, we will only assume that the long time behavior of $\tilde{F}_2(t/\tau_s)$ reflects solely polymer contributions**:**

$$\lim_{t \geq \tau_e \gg \tau_s} \tilde{F}_2(t/\tau_s) = \tilde{F}_{polymer}(t/\tau_s) \quad (2)$$

Here τ_e denotes the time scale beyond which entanglement effects are felt by the polymer segment. Whether eq 2 indeed holds can be checked by comparing $\tilde{F}_2(t/\tau_s)$ with that for $M < M_R$representing solely the contribution from glassy dynamics.

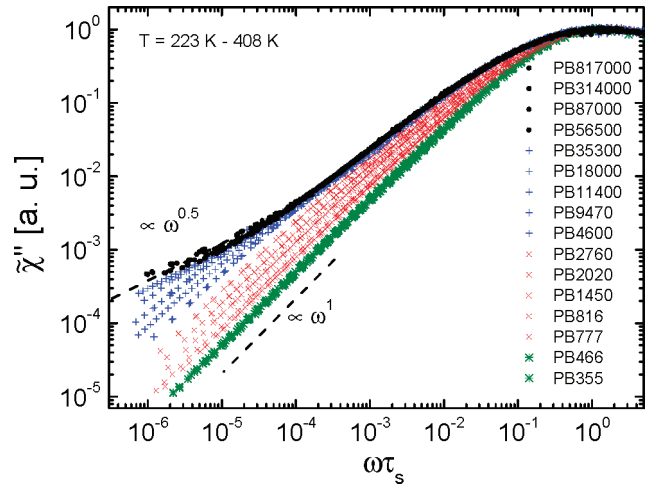

Figure 1. Susceptibility master curves for a series of polybutadienes (PB) with molecular weight (M) as indicated: (green stars) $M = 466$ represents simple liquid behavior; (red crosses) polymers showing only Rouse dynamics; (blue +) polymers showing in addition entanglement dynamics with crossover to terminal relaxation; (black circles) high M limit.

Within a coarse grained description and certain assumptions concerning the nature of the stochastic process,[14,17] the correlation function $F_{polymer}(t)$ may be related to the square of the tangent or bond vector correlation function $\phi_b(t) = \langle \boldsymbol{u}_b(0)\boldsymbol{u}_b(t)\rangle$, i.e.,

$$F_{polymer}(t) \cong \phi_b(t)^2 \quad (3)$$

where $\boldsymbol{u}_b$ is a unit vector along the contour of the polymer chain. Equation 3 offers the possibility to convert the T_1 dispersion data into the bond vector correlation function which is accessible also by simulation studies.[12,13] This is also the route for calculating T_1 from theory like the Rouse model.[9,14,17] We note that eq 3 has been tested for simulation vs experiment and some differences have been found.[13]

3. Experimental Section

We have investigated samples of 1,4-polybutadiene (PB) of different molecular weight M (see Table 1) in order to complete the M range of our study between the low (PB466) and the high (PB817000) M from refs 8 and 9. Note that the sample names reflect M_w (weight averaged M). The samples were purchased from Polymer Standards Service PSS, Mainz, Germany.

The dispersion of the spin−lattice relaxation time T_1 has been determined with a STELAR relaxometer FFC 2000, which allows measurements in the temperature range of 200−410 K and ^{1}H Larmor frequency range $\nu = 10$ kHz to 20 MHz. The accuracy of temperature measurements was better than ±1 K, while the temperature stability was better than ±0.3 K. We have observed simple exponential relaxation of magnetization over at least an order of magnitude in magnetization, and thus have determined the time constant T_1 by fitting to the exponential function. For further details, see refs 8 and 9.

4. Results

Susceptibility Master Curves. In Figure 1, we compile our results for the NMR susceptibility master curves $\tilde{\chi}''(\omega\tau_s)$ of PB in the molecular weight range $355 < M < 817000$ including our previous[8,9] as well as our new data (cf. Table 1). Typical dispersion data $T_1(\omega)$ of PB have been presented in ref.[8,9] The curves in Figure 1 are plotted as a function of the reduced frequency $\omega\tau_s$ where τ_s is the segmental correlation time which

we identify with that of the glass transition τ_α. The master curves have been constructed as described in ref 8 (cf. also Theoretical Background). Applying FTS, the master curves contain all the relaxation data for a given M measured in the temperature range 223−408 K and thereby we significantly enlarge the frequency range extending over more than 6 decades below $\omega\tau_s \cong 1$. The molecular weights chosen include the low M limit (PB355 and PB466, green stars) as well as the high M limit ($M \geq 56500$, black circles). In the latter case the dispersion of T_1 is independent of M. In this contribution we focus on the crossover from Rouse to entanglement dynamics $M > M_e$ which was not systematically covered by our previous works.[8,9]

As demonstrated before,[9] in the Rouse regime $M < 4600$ (red crosses in Figure 1), the dispersion data can be described by applying the discrete Rouse model with only a few Rouse modes being activated provided that the contributions of glassy and polymer dynamics are separated. The corresponding susceptibility curves at $\omega\tau_s \ll 1$ show excess intensity with respect to the spectrum of the low M limit (PB355 or PB466) which exhibits Debye behavior $\tilde{\chi}''(\omega) \propto \omega^1$ typical of simple liquids.[8,9] First polymer effects show up at $M = 777$ and the excess intensity grows until it saturates around $M = 4600$. In all cases, a Debye limit is reached at lowest frequencies indicating that the terminal relaxation can be probed in the Rouse regime.

At $4600 \leq M \leq 18000$ the master curves (blue + symbols) show discernible bimodal character which indicates the presence of entanglement dynamics. Whereas the relaxation behavior is not changed for $\omega\tau_s > 10^{-4}$ with respect to that of PB with $M < 4600$, more and more additional intensity appears at frequencies $\omega\tau_s < 10^{-4}$ signaling a further retardation of the segmental dynamics due to entanglement effects. We have explained the saturation behavior for $\omega\tau_s > 10^{-4}$ by the fact that the number of Rouse modes cannot grow any longer when M_e is reached.[9] Note that up to $M = 18000$ a crossover to the Debye limit is still probed at lowest frequencies $\omega\tau_s = 10^{-7} - 10^{-6}$, i.e. the terminal relaxation is reached even for the onset of the entanglement regime. In the case of $M = 35300$ indication of this crossover is still discernible, however, the final Debye limit is not reached. At $M > 35300$ the crossover to the terminal relaxation is not observed at all, and the corresponding susceptibility curves display an M independent relaxation behavior (high M limit, black circles).

Reorientational Correlation Function. As an alternative way of presenting NMR data, one may Fourier transform the spectra $\tilde{\chi}''(\omega\tau_s)$ into the corresponding segmental orientational correlation functions $\tilde{F}_2(t/\tau_s)$.[9] Such transformation is only possible for spectral data that show the limiting $\propto \omega^1$ behavior at lowest frequencies, i.e. for the case that the terminal relaxation is reached. As said, for $M \leq 18000$ this condition is fulfilled, and the corresponding correlation functions are displayed in Figure 2. They are monitored over 6 decades in amplitude and up to 8 decades in reduced time t/τ_s. As we focus on the crossover from Rouse to entanglement dynamics we only show data for $M \geq 2760$. For comparison we include the corresponding correlation function for the simple liquid limit (PB466); it is interpolated by a Kohlrausch decay with a stretching parameter $\beta_K = 0.4$, a behavior typical of low molecular weight glass formers.[3,4] As in the case of the susceptibility data in Figure 1, in going from $M = 2760$ to $M = 18000$, the correlation functions display more and more bimodal character with a distinct shoulder at long times; i.e., full reorientational relaxation of a segment is increasingly retarded due to the entanglement dynamics strongly depending on M. Although the reorientational correlation function shows a bimodal shape a clear-cut plateau region as anticipated in several works[16] is not recognized. It is obvious that the correlation function of glassy dynamics given by that of PB466 does not provide contributions at times $t/\tau_s > 10^2$, i.e., at time scales relevant to entanglement dynamics.

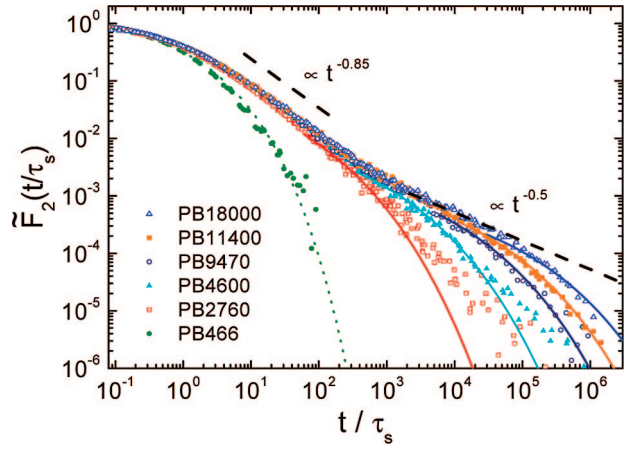

Figure 2. Dipolar or reorientational correlation functions $\tilde{F}_2(t/\tau_s)$ obtained from the data in Figure 1 via Fourier transformation for $M \geq 2760$ and for comparison $M = 466$. Dotted line: fit by Kohlrausch decay. Solid lines: estimating the terminal decay. Dashed lines: apparent power law $t^{-0.85}$ at short times, and $t^{-0.5}$ at long times for high M limit.

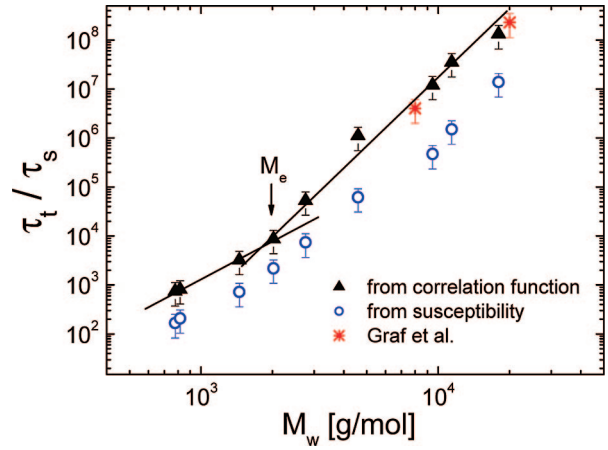

Figure 3. M dependence of the reduced terminal relaxation time τ_t/τ_s assuming a Kohlrausch decay ($\beta_K = 0.25$) at long times (black triangles) compared with corresponding data obtained from analyzing the susceptibility master curves (blue circles);[9] data from Graf et al.[16] assuming that DQ NMR probes the terminal relaxation (red stars).

The correlation functions in Figure 2 exhibit a common behavior at times shorter than say $t/\tau_s < 3\times10^2$ which comprises contributions from Rouse as well as glassy dynamics and an apparent power law behavior $t^{-0.85}$ can be identified (dashed line in Figure 2). At $t/\tau_s > 3\times10^2$, additional contributions from entanglement dynamics set in which appear to form an M independent envelope, i.e., the higher M the later the final decay associated with the terminal relaxation and fixed by a time constant τ_t sets in. Assuming a stretched exponential terminal relaxation ($\beta_K = 0.25$) allows us to estimate the M dependence of τ_t. Technically, we determine τ_t by the time when the derivative of the correlation function becomes −1 in a double logarithmic plot. The corresponding interpolation of the decay curves are shown in Figure 2. It provides only an approximation in particular at small M for which the terminal relaxation is difficult to identify.

Figure 3 presents the time constant τ_t as a function of M, and the results for lower M (Rouse regime) are also included (black triangles). A crossover from a power law behavior $\tau_t \propto M^{2.5 \pm 0.8}$ to $\tau_t \propto M^{4.5 \pm 0.7}$ around $M \cong 2000$ emerges, which is in fair agreement with expectations for Rouse and entanglement dynamics, respectively.[1] This fixes the entanglement molecular

Table 2. Predictions of the Tube-Reptation Model for the Mean Square Segment Displacement $\langle r^2(t)\rangle$,[1] NMR Susceptibility $\chi''(\omega)$,[14] Reorientational Correlation Function $F_2(t)$,[22] and Bond Correlation Function $\phi_b(t)$ (assuming $F_2(t) = \phi_b^2(t)$ cf. eq 3)

regime	limit	$\langle r^2(t)\rangle$	$\chi''(\omega)$	$F_2(t)$	$\phi_b(t)$
II (free Rouse)	$\tau_s \le t \le \tau_e$	$M(t/\tau_R)^{0.5} \propto (t/\tau_s)^{0.5}$	$\omega\tau_s \ln(\omega\tau_s)$	$(t/\tau_s)^{-1}$	$(t/\tau_s)^{-0.5}$
III	$\tau_e \le t \le \tau_R$	$M(t/Z^2\tau_R)^{0.25} \propto (t/\tau_s)^{0.25}$	$(\omega\tau_s)^{0.25}$	$(t/\tau_s)^{-0.25}$	$(t/\tau_s)^{-0.125}$
IV	$\tau_R \le t \le \tau_d$	$M(t/\tau_d)^{0.5} \propto M^{-0.5}(t/\tau_s)^{0.5}$	$M^{+0.5}(\omega\tau_s)^{0.5}$	$M^{+0.5}(t/\tau_s)^{-0.5}$	$M^{+0.25}(t/\tau_s)^{-0.25}$
V	$\tau_d \ll t$	$M(t/\tau_d)^1 \propto M^{-2}(t/\tau_s)^1$	$(\omega\tau_s)^1$	e^{-2t/τ_d}	e^{-t/τ_d}

weight to $M_e \cong 2000$ as found before.[9] This M value is actually by a factor of about two smaller than that value for which saturation in the frequency regime $\omega\tau_s > 10^{-4}$ (attributed to Rouse dynamics) occurs in Figure 1. The results also agree fairly well with those obtained previously from analyzing the terminal relaxation in the susceptibility representation (blue circles in Figure 3).[9] Given this, it becomes clear from Figure 2 that up to $M = 18000$ (corresponding to $Z = M/M_e \cong 9$) a significant part of the correlation function is dominated by the terminal relaxation leading to a cutoff of the characteristic polymer relaxation. It appears that the terminal relaxation is the only M dependent feature of the correlation function. Thus, it will not be easy identifying presumably universal polymer relaxation (cf. Discussion).

5. Discussion and Conclusions

Extending our previous measurements on PB[8−10] we constructed master curves for the susceptibility $\tilde{\chi}''(\omega\tau_s)$, and via Fourier transformation one arrives at the dipolar or segmental correlation function $\tilde{F}_2(t/\tau_s)$ of entangled polymers ($M > M_e$) monitored up to 8 decades in reduced time t/τ_s (cf. Figure 2). This function is not easily obtained by other experiments, and most simulation data do not cover sufficient time or amplitude to allow for a detailed discussion of its properties in the entanglement regime. We reiterate that the result for $\tilde{F}_2(t)$ and $\phi_b(t)$ depends only on applying FTS which is accepted as a good approximation; if deviations are reported they are small on logarithmic scales. Note also that for the discussion we can ignore the difference between $\tilde{F}_2(t)$ and $F_2(t)$ (*cf.* eq 1).

Testing Theoretical Predictions for Polymer Dynamics. At first, we will discuss our result for $\tilde{F}_2(t/\tau_s)$ (cf. Figure 2) in the light of theoretical predictions within coarse grained descriptions of polymer dynamics, i.e., molecular details of the monomer are ignored.[1,14,18−22] We only note that atomistic simulations have accessed the segmental correlation function $F_2(t)$ for PB[23−25] as well as PI[26] and qualitatively similar relaxation curves have been found, in particular, the decay curves show a bimodal structure as in our experiment.

The segmental correlation function $\tilde{F}_2(t/\tau_s)$ is expected to reflect five contributions: regime I, glassy dynamics $t \le \tau_s$; regime II, virtually free Rouse dynamics $\tau_s < t \le \tau_e$, for which entanglement effects are not yet effective. Here, $\tau_e = \tau_s N_e^2$ denotes the entanglement time and N_e the number of Rouse units forming an entanglement unit. The time τ_e marks the crossover to dynamics governed by entanglement effects. Here, according to the tube-reptation model[1] three distinct regimes have to be further distinguished which lead to characteristic power law behavior for the mean square displacement and the dispersion of $T_1(\omega)$.[14,18,22] At $\tau_e \le t \le \tau_R$, curvilinearly directed Rouse dynamics (III) occur in the fictitious tube by which a tagged polymer chain is fixed due to being entangled with other polymers. The time constant $\tau_R = \tau_s N^2$ specifies the longest Rouse time. The interval $\tau_R \le t \le \tau_d$ defines the diffusion process along the tube (IV) which is terminated by the tube disengagement (or disentanglement) time $\tau_d = 3\tau_s N^3/N_e$; i.e., this terminal relaxation is strongly M dependent. Finally, at $t \gg \tau_d$, translational diffusion and isotropic reorientation of the entire polymer (V) take place, and a Debye limit for the dispersion of T_1 is reached.

Table 3. Predictions of the (first) Renormalized Rouse Model for Mean Square Segment Displacement $\langle r^2(t)\rangle$,[14] NMR Susceptibility $\chi''(\omega)$,[14] Reorientational Correlation Function $F_2(t)$ and Bond Correlation Function $\phi_b(t)$ (assuming $F_2(t)=\phi_b^2(t)$ cf. eq 3)

regime	limit	$\langle r^2(t)\rangle$	$\chi''(\omega)$	$F_2(t)$	$\phi_b(t)$
"high-mode number limit"	$\tau_s \le t$	$(t/\tau_s)^{0.25}$	$(\omega\tau_s)^{0.5}$	$(t/\tau_s)^{-0.5}$	$(t/\tau_s)^{-0.25}$
"low-mode number limit"	$\tau_e \le t$	$(t/\tau_s)^{0.4}$	$(\omega\tau_s)^{0.8}$	$(t/\tau_s)^{-0.8}$	$(t/\tau_s)^{-0.4}$

Regarding the tube-reptation model, Table 2 compiles the results for the respective power law regimes of the mean square segment displacement $\langle r^2(t)\rangle$,[1] the NMR susceptibility $\chi''(\omega\tau_s)$,[14,18] the segmental reorientational correlation function $F_2(t/\tau_s)$,[22] and the bond vector correlation function $\phi_b(t/\tau_s)$ (cf. below). We emphasize that regimes I−III show no M dependence, i.e., universal envelopes are forecast for $\chi''(\omega\tau_s)$ or $F_2(t/\tau_s)$, whereas for regimes IV−V such dependence is predicted.

Referring to the free Rouse regime (II), a comment is worthwhile. As demonstrated in our previous Paper,[9] the power law expression $\tilde{F}_2(t) \propto t^{-1}$ typical of this regime (cf. Table 1) is actually only observed in the high N limit, e.g., above $N = 10^2$. This behavior is not found in real polymers for which entanglement effects set in well before this limit is reached. Instead of testing the expected limiting behavior, one rather has to perform a discrete Rouse analysis, summing up a small number of Rouse modes.[9] In Figure 2 we attribute the relaxation behavior at $t/\tau_s < 3\times10^2$ to glassy and Rouse dynamics with a few modes being active only. The behavior in this time range is essentially the same as that of the polymer with $M = 2760$ which is only slightly above M_e, thus not expected to show significant entanglement dynamics. Here, an apparent power law $\tilde{F}_2(t) \propto t^{-a}$ with $a = 0.85$ may be identified over 2 decades in time, which actually is not much different from that of the Rouse limit $a = 1$.

At $t/\tau_s > 3\times10^2$ the reorientational correlation function for the different $M > M_e$ follows more and more an M independent envelope. Beyond $M = 18000$, i.e., $Z \cong 9$, no full correlation function is available by Fourier transformation of the dispersion data. Instead, we include in Figure 2 the Fourier transform of the power law limit of the susceptibility (dashed line) observed at lowest frequencies in Figure 1 for $M > 18000$, i.e., for the high M limit. The corresponding exponent is $a = 0.5 \pm 0.05$. For $M \le 18000$ the segmental correlation function is terminated by a Kohlrausch decay with a terminal time τ_d which follows the predicted M behavior (cf. Figure 3).

The results of Figure 2 are in stark contrast to the theoretical predictions of the tube-reptation model (*cf.* Table 2). The power law of regime III with an exponent $a = 0.25$ is not observed. The second power law of the tube-reptation model (regime IV) with an exponent $a = 0.5$ could be identified with the experimental one at longest times; however, the corresponding M dependence is missing. As said before, it appears that for the M range covered an M dependence of the segmental correlation function is only introduced by that of the terminal relaxation; i.e., for $t \ll \tau_d$, no M dependence is observed in contrast to the prediction.

As an alternative description of the dynamics of entangled polymers, the renormalized Rouse model[20,21] is discussed by the Kimmich group.[14,17,19] The corresponding power law predictions are compiled in Table 3. We note that a "free Rouse" regime is not expected within this approach. Before discussing

their interpretation we emphasize that the experimental T_1 dispersion data of PB compiled by us agree with those of the Kimmich group.[27] The authors have claimed that the two power laws of Table 3 are observed in the T_1 dispersion data (accepting an error of ±0.05 in the exponents[14]). The first regime at high frequencies, the "high mode number limit", should be described by a power law $\tilde{F}_2 \propto (t/\tau_s)^{-0.5}$ at short times. In the NMR data of Figure 2 such a behavior appears only at longest times. Regarding the second power law regime ("low mode number limit") with $a = 0.8$, indeed, this is approximately revealed but we attribute it to the Rouse regime (*cf.* dashed line with $a = 0.85$). The experimentally observed behavior at longest times described by $\tilde{F}_2 \propto (t/\tau_s)^{-0.5}$, for which the contribution of glassy dynamics can safely be ignored, is attributed by Kimmich et al. to the "inter-segment interaction limit".[14] This identification has become possible by comparing ^{1}H and ^{2}H dispersion data.[27] The ^{2}H relaxation is dominated by quadrupolar interaction probing only intra segmental fluctuations whereas ^{1}H relaxation may contain intermolecular correlation effects, in addition (see Note Added in Proof).

We would also like to compare our results with those from double quantum (DQ) NMR experiments on PB[16,28,29] where similar correlations are probed as in FFC NMR. The authors have analyzed their data in terms of power laws of regime III and IV of the tube-reptation model. In this study entangled PB with $Z = 4$, 11, 76 has been investigated and no terminal relaxation has been considered. In the present contribution, assuming $M_e = 2000$, we clearly identify the terminal relaxation for $Z \leq 9$ (cf. Figure 2) and cover similar time scales as the DQ NMR experiments. Thus, it may be possible that the decay curves observed in the DQ NMR experiments actually reflect the terminal relaxation instead of different power law regimes. We have interpolated the DQ NMR decay curves of ref 16 by assuming a stretched relaxation, and indeed we find for the samples with the two lowest Z values, *i.e.*, $Z = 4$ ($M = 8000$) and $Z = 11$ ($M = 20000$), a similar M dependence as in our case for the terminal relaxation in the entanglement regime (cf. Figure 3); the very slow DQ decay curve for the highest M ($Z = 76$) studied cannot be reliably interpolated. For a quantitative comparison of the FFC and DQ results one has to assume $\tau_e/\tau_s = 5 \times 10^5$, which is a reasonable value. Here, we note that in a very recent study on PB, Saalwächter and co-workers have been able to study significantly higher M values over a larger time window, and they have indeed identified the power laws of the tube-reptation model.[30]

Bond Vector Correlation Function. As mentioned in section 2, within theoretical approaches for coarse grained polymer dynamics the correlation function $F_2(t/\tau_s)$ is given by the square of the bond vector correlation function $\phi_b(t)$ (*cf.* eq. 3).[14,15,17] Therefore we plot $\phi_b(t)$ in Figure 4 obtained from the data in Figure 2. Qualitatively, the relaxation behavior does not change significantly with respect to that of $\tilde{F}_2(t)$. Of course, the corresponding exponents decrease by a factor of 2. Studying the crossover from Rouse to reptation dynamics Kreer et al.[12] have investigated the bond vector correlation function by Monte Carlo simulations. The authors have stated that the "crossover from non-entangled to entangled dynamics is very protracted". Even for longest chains ($N = 512$) they have not found evidence of the power laws expected for tube-reptation dynamics. Moreover, no difference is observed for $N = 128$, and $N = 512 = 14N_e$; i.e., the bond vector correlation function appears to be N independent over 7 decades in time. We have included in Figure 4 (solid lines) the results from the simulation study[12] (multiplied by a factor 2π in time). The curves for $N = 128$ and $N = 512$, which do not differ within the scatter of the data, exhibit high similarity compared to the FFC NMR results for highest $M = 18000$. Even the simulation data for the other N

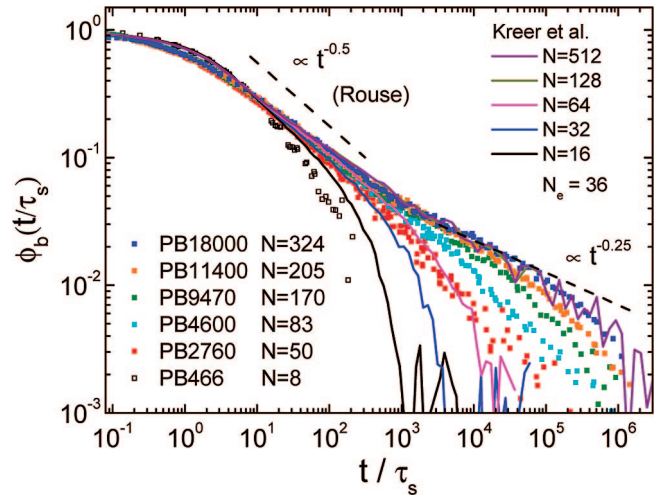

Figure 4. Bond vector correlation function $\phi_b(t/\tau_s) = F(t/\tau_s)^{1/2}$ as obtained from the T_1 dispersion data. Solid lines: data from Monte Carlo simulations by Kreer et al.;[12] given $N_e = 36$ and $M_e = 2000$, experiments and simulations are mapped onto each other; dashed lines: power law regimes.

can be mapped to the experimental ones when taking $N_e = 36$ (simulations) and $M_e = 2000$ (our experiment). Simulation as well as experiment get close to the Rouse limit $t^{-0.5}$ at times $1 < t/\tau_s < 3 \times 10^2$. At even shorter times, for which contributions from glassy dynamics dominate, small deviations between experiment and simulation are observed which, of course, are expected within coarse grained models. All in all, the similarity of both results is very striking, in particular, given that we expect also inter segmental contributions at long times,[14] which are not included in the simulation. Moreover, the relaxation strength of the polymer relaxation is expected to depend on the structural details within the monomer.[28] Therefore, we think that the coincidence may be accidental.

Concluding, our results for the bond vector and segmental correlation function confirm the findings from simulation which do not show the crossover to the relaxation behavior predicted for these quantities by the standard polymer theories like the tube-reptation model up to values $Z \cong 9$. Of course, it may be possible that the crossover is only observed at even higher Z or M which then makes it necessary to study the dynamics up to even longer times. This view is supported by the mentioned observations in a recent DQ NMR study of PB.[30] As discussed, e.g., by Read et al, contour length fluctuations and constraint release may play an important role.[31] In any case, FFC NMR provides a unique opportunity for elucidating dynamics in polymer systems and indeed longer time scales may become feasible when stray field compensation is optimized.

Acknowledgment. The authors thank J. Baschnagel (Institute Charles Sadron, Strasbourg, France) for providing the simulation data, and H.W. Spiess (Mainz, Germany) and K. Saalwächter (Halle, Germany) for helpful comments on the manuscript. The authors also appreciate financial support of Deutsche Forschungsgemeinschaft (DFG) through SFB 481. V.N.N. acknowledges support by the RFBR.

Note Added in Proof. We mention that within the twice renormalized Rouse model the inter-segmental correlation function is described by a power law $t^{-0.5}$ (see ref 32) as found experimentally at longest times.

References and Notes

(1) Doi, M.; Edwards, S. F. *The Theory of Polymer Dynamics*; Oxford Sci. Publication: Oxford, U.K., 1986.

(2) Angell, C. A.; Ngai, K. L.; Mckenna, G. B.; McMillan, P. F.; Martin, S. W. *J. Appl. Phys.* **2000**, *88*, 3113–3157.
(3) Lunkenheimer, P.; Schneider, U.; Brand, R.; Loidl, A. *Contemp. Phys.* **2000**, *41*, 15–36.
(4) Blochowicz, T.; Brodin, A.; Rössler, E. A. *Adv. Chem. Phys.* **2006**, *133 Part A*, 127–256.
(5) Binder, K.; Baschnagel, J.; Paul, W. *Prog. Polym. Sci.* **2003**, *28*, 115–172.
(6) Paul, W.; Smith, G. D. *Rep. Prog. Phys.* **2004**, *67*, 1117–1185.
(7) Götze, W.; Sjögren, L. *Rep. Prog. Phys.* **1992**, *55*, 241–376.
(8) Kariyo, S.; Brodin, A.; Gainaru, C.; Herrmann, A.; Schick, H.; Novikov, V. N.; Rössler, E. A. *Macromolecules* **2008**, *41*, 5313–5321.
(9) Kariyo, S.; Brodin, A.; Gainaru, C.; Herrmann, A.; Hintermeyer, J.; Schick, H.; Novikov, V. N.; Rössler, E. A. *Macromolecules* **2008**, *41*, 5322–5332.
(10) Kariyo, S.; Gainaru, C.; Schick, H.; Brodin, A.; Rössler, E. A. *Phys. Rev. Lett.* **2006**, *97*, 207803-1−207803-4. Erratum: Kariyo, S.; Herrmann, A.; Gainaru, C.; Schick, H.; Brodin, A.; Rössler, E. A. *Phys. Rev. Lett.* **2008**, *100*, 109901-1.
(11) Hintermeyer, J.; A. Herrmann, A.; Kahlau, R.; Goiceanu, C.; Rössler, E. A. *Macromolecues* **2008**, *41*, 9335–9344.
(12) Kreer, T.; Baschnagel, J.; Müller, M.; Binder, K. *Macromolecules* **2001**, *34*, 1105.
(13) Sommer, J.-U.; Saalwächter, K. *Eur. Phys. J. E* **2005**, *18*, 167–182.
(14) Kimmich, R.; Fatkullin, N. *Adv. Polym. Sci.* **2004**, *170*, 1–113.
(15) Bloembergen, N.; Purcell, E. M.; Pound, R. V. *Phys. Rev.* **1948**, *73*, 679–715.
(16) Graf, R.; Heuer, A.; Spiess, H. W. *Phys. Rev. Lett.* **1998**, *80*, 5738–5741.
(17) Fatkullin, N.; Kimmich, R.; Weber, H. W. *Phys. Rev. E* **1993**, *47*, 4600–4603.
(18) de Gennes, P.-G. *J. Chem. Phys.* **1971**, *55*, 572–579.
(19) Kimmich, R.; Fatkullin, N. *J. Chem. Phys.* **1994**, *101*, 822–832.
(20) Schweizer, K. S. *J. Chem. Phys.* **1989**, *91*, 5802–5821.
(21) Schweizer, K. S. *J. Chem. Phys.* **1989**, *91*, 5822–5839.
(22) Ball, R. C.; Callaghan, P. T.; Samulski, E. T. *J. Chem. Phys.* **1997**, *106*, 7352.
(23) Faller, R.; Müller-Plathe, F.; Heuer, A. *Macromolecules* **2000**, *33*, 6602–6610.
(24) Smith, G. D.; Borodin, O.; Bedrow, D.; Paul, W.; Qiu, X.; Ediger, M. *Macromolecules* **2001**, *34*, 5192–5199.
(25) Smith, G. D.; Borodin, O. *J. Chem. Phys.* **2002**, *117*, 10350.
(26) Faller, R.; Müller-Plathe, F. *Polymer* **2002**, *43*, 621–628.
(27) Kimmich, R.; Fatkullin, N.; Seiter, R.-O.; Gille, K. *J. Phys. Chem.* **1998**, *108*, 2173–2177.
(28) Dollase, T.; Graf, R.; Heuer, A.; Spiess, H. W. *Macromolecules* **2001**, *34*, 298–309.
(29) Saalwächter, K. *Progr. NMR* **2007**, *51*, 1–35.
(30) Saalwächter, K. Private communication.
(31) Read, D. J.; Jagannathan, K.; Likhtman, A. E. *Macromolecules* **2008**, *41*, 6843–6853.
(32) Fatkullin, N.; Kimmich, R.; Kroutieva, M. *J. Exp. Theor. Phys.* **2000**, *91*, 150–166.

MA802818J